Food Innovation and Advances

ARTICLE

Open Access

https://doi.org/10.48130/fia-0024-0021

Food Innovation and Advances **2024**, 3(3): 222–231

Protection mechanism of β-carotene on the chlorophyll photostability through aggregation: a quantum chemical perspective

Fangwei Li[1,2,3], Suxia Shen[1,2], Zhaotian Yang[1,2], Jinghao Zhang[1,2], Ajibola Nihmot Ibrahim[1,2] and Yan Zhang[1,2*]

[1] *College of Food Science and Nutritional Engineering, China Agricultural University, Beijing 100083, People's Republic of China*
[2] *National Engineering Research Center for Fruit and Vegetable Processing, Ministry of Science and Technology, Beijing 100083, People's Republic of China*
[3] *College of Food Science and Engineering, Ocean University of China, Qingdao 266003, People's Republic of China*
* Corresponding author, E-mail: zhangyan348@163.com

Abstract

Chlorophyll (Chl), the most widely distributed natural pigment in nature, is limited in use due to its poor stability. This study refers to the aggregation structure of Chl and carotene (Car) in natural photosynthetic systems, hoping to improve the photostability of Chl by constructing Chl/Car aggregates. The stability protection effect of Car on Chl was explored by designing different ratios of Chl and Car aggregation systems. The configuration of Chl/Car aggregates was optimized through ab initio molecular dynamics, and the aggregation mechanism of the aggregates and the photoprotection mechanism of Chl by Car were elucidated through quantum chemical calculations and wave function analysis. Chl/Car had a 27.22% higher Chl retention rate than free Chl after 7 d of illumination, with a Chl to Car ratio of 1.66:1. A configuration of the Chl/Car aggregates which Car's conjugated olefin chain interacts extensively with the porphyrin ring and bent phytyl chain of Chl made them more stable. The photoprotective mechanism of Car on Chl in the Chl/Car aggregates is elucidated. Car's conjugated polyene chain provides HOMO orbitals to the Chl/Car aggregates. It demonstrated that Car supplies electrons in the low-lying excited states S2 and S4, indicating it is more susceptible to damage, protecting Chl. This research will promote the development of natural color formulas and ensure the health of consumers.

Citation: Li F, Shen S, Yang Z, Zhang J, Ibrahim AN, et al. 2024. Protection mechanism of β-carotene on the chlorophyll photostability through aggregation: a quantum chemical perspective. *Food Innovation and Advances* 3(3): 222–231 https://doi.org/10.48130/fia-0024-0021

Introduction

Chlorophyll (Chl) has become one of the most important natural food pigments because of its rich and numerous sources and pleasant color. Usually, chlorophyll is extracted from algae and vegetables[1]. It has been confirmed that Chl demonstrates excellent properties in antioxidant, antimutagenic, anti-inflammatory, and weight loss aspects[2,3]. However, the stability of Chl during food processing is affected by factors including heat, light, oxygen, acid, and enzymes[4,5]. The stability exhibits a high degree of sensitivity to these factors, leading to its degradation and discoloration. Light and heat are among the most prevalent factors that constrain its applications.

Upon exposure to light, Chl molecules are excited from their ground state to an excited state, transforming into potent oxidizing agents. Subsequently, they interact with surrounding environmental components, resulting in the destruction of their structural integrity[6]. To date, the chemical methods employed in food processing to mitigate Chl degradation primarily encompass regulating pH and ionic strength, inhibiting the activity of chlorophyllase enzymes, supplementing antioxidants, and incorporating salts (like Cu^{2+} or Zn^{2+} salts) for re-greening purposes, among various other strategies[7–9]. Salting and re-greening is one of the most widely adopted methods. It converts Chl into metal chlorophyll complexes, like copper sodium chlorophyllin, which can exhibit a similar green color to natural Chl and have less susceptibility to acid and heat, thus enhancing its stability. Similar to natural chlorophyll, the detachment of the central metal ion under acidic conditions and heat treatment is the most prevalent structural alteration in copper sodium chlorophyllin. On the other hand, using synthetic pigments in food may harm human health. Research has shown that it poses risks of symptoms such as hyperactivity, irritability, sleep disorders, increased aggression, and allergies[10,11]. Overall, the chemical methods, whether introducing new substances into the original food or altering the original structure of Chl, are insufficient as universally applicable protective methods for various Chl-rich raw materials in future processing or storage.

In the photosynthetic system of plants, Chl and beta-carotene (β-Car) are essential components that coexist in the light-harvesting complexes[12]. They work together to absorb light energy and transfer it to the reaction center. In addition to β-Car, other carotenoids such as lutein, violaxanthin, and neoxanthin are also present around Chl in the plant's photosynthetic system[13]. Plants form this natural coexistence relationship during their long-term evolutionary adaptation process to dissipate excess light energy. It is a synergy between Chl and Car through energy transfer and response to the surrounding environment, enabling the photosynthetic system to operate efficiently and stably[14]. When photosystem II (PSII) is exposed to intense light, Chl becomes excited and transitions to its triplet state. It then reacts with oxygen, producing harmful reactive oxygen species[15]. Meanwhile, the chemical structure of Chl gets damaged due to exposure to light and oxygen. Chl undergoes irreversible decomposition under the influence of

ultraviolet and visible light, resulting in the formation of derivatives. Singlet oxygen participates in the degradation of Chl under illumination, and the photooxidation of the porphyrin ring structure ultimately leads to the formation of colorless products[16]. The plant's photoprotection mechanisms safeguard the stability of the photosynthetic system, with β-Car playing a pivotal role in this process. There is energy transfer between Chl and Car, which helps in quenching the excitation of Chl and maintaining the stability of the photosynthetic system[15,17]. Car possess more than 11 conjugated double bonds in their structure. They can absorb excess light energy and dissipate it through polyene vibrations, which can directly quench the singlet excited state of Chl and scavenge singlet oxygen ($_1O^2$)[18]. The natural aggregation forms of Chl and Car can serve as a reference for constructing Chl/Car aggregates, offering a promising approach to enhance the stability of Chl.

Analogous to the production of reactive oxygen species (ROS) during photosynthesis in photosynthetic organisms, animal and human respiratory metabolism also continually generate ROS. When the concentration of ROS is high, it can cause oxidative damage to biomolecules such as cellular lipids, proteins, and DNA, leading to chronic inflammation. This continuous generation of ROS can contribute to the development of various diseases, including cancer, lung diseases, and autoimmune disorders[19]. Carotenoids have gained significant attention due to their potent antioxidant, photoprotective, coloring, and physiological activities. Carotenoids have extensive applications spanning the food, healthcare, skincare and cosmetics, pharmaceutical, and animal feed industries, playing a vital role in sustaining organisms' ongoing health and vitality.

In this study, the proportion of Chl and Car was modeled after the natural photosynthetic system, with the research primarily focusing on the photoprotective role of Car in safeguarding Chl through aggregation. The weak interactions and mechanisms between Car and Chl and their impact on coloring properties were studied. Utilizing a quantum chemical approach, the weak interactions between Chl and Car were elucidated through an in-depth analysis of their molecular structures and wave functions. The outcomes of this research will facilitate the development of more natural color formulations, thereby enhancing the quality of food products while ensuring the health and safety of consumers.

Materials and methods

Extraction and purification of Chl

The spinach used in the experiment was purchased from the vegetable market of China Agricultural University (Beijing, China). The extraction and purification method for Chl referenced the method of Cao et al.[4] with slight modifications. Fresh spinach was weighed to 200 g after removing stems and veins. The weighed spinach was put in a blender, and 200 mL of anhydrous ethanol and 400 mL of petroleum ether were added. The mixture was blended for 5 min to achieve a uniform viscous liquid consistency. The blended sample was then subjected to cold centrifugation at 4 °C and 8,000× g for 10 min. The supernatant was collected and filtered. The filtrate was transferred to a separating funnel, and an equal volume of water was added. The mixture was shaken and allowed to separate. The lower aqueous phase (ethanol-water mixture) was removed, while the upper organic phase (petroleum ether layer) was retained. This washing step was repeated two more times with equal volumes of water. After collecting the organic phase, it was dried using anhydrous sodium sulfate and filtered. The sample was then transferred to a rotary evaporator and evaporated at 36 °C until the remaining volume was approximately 200 mL, resulting in crude Chl extract. The crude Chl extract was subjected to column chromatography using neutral alumina as the stationary phase. The elution was performed sequentially using petroleum ether-acetone (v:v = 9:1), petroleum ether-acetone (v:v = 7:3), and n-butanol-ethanol-water (v:v:v = 3:1:1) as eluents to separate and elute carotenoids, xanthophylls, and Chl. The eluted Chl fraction (purity 86.6%) was collected and kept for further use.

Experimental program

The β-Car used in this study was of analytical grade and purchased from Shanghai Yuanye Biotechnology Co., Ltd (Shanghai, China). For the whole experiment, Chl and β-Car were mixed in an ethanol solution to create samples A, B, C, D, E, and F, with a constant Chl concentration of 19.93 mg/L and β-Car concentrations of 1.20, 2.40, 3.60, 4.80, 6.00, and 7.20 mg/L, respectively. Two control samples, G (Chl 19.93 mg/L) and H (β-Car 3.60 mg/L), were also prepared. These eight samples were subsequently placed at room temperature, with the experimental environment maintaining a constant light intensity of approximately 2,000 lux for 24 h a day. Changes in the indicators on the 7th day and the 70th day of the light treatment were recorded. Among them, the data from the 7th day was used to analyze the protective phenomenon of Car on Chl, while the data from the 70th day was employed to analyze the mechanism of Car's protective effect on Chl.

Determination of Chl content

The Chl content was determined based on Toprak's method with minor modifications[20]. After the Chl sample had been appropriately diluted, 200 μL was poured into a 96-well plate, and the absorbance was measured at 645 and 663 nm using a spectrophotometer (SpectraMax iD5, Molecular Devices, USA). All experiments were conducted under light-shielded conditions. Based on the absorbance, the chlorophyll content was calculated using the following formula:

$$\text{Chl concentration (mg/L)} : C = 8.04 \times A_{663} + 20.29 \times A_{645} \quad (1)$$

Determination of fluorescence spectrum

The fluorescence measurements of the Chl solution were conducted using a spectrophotometer (SpectraMax iD5, Molecular Devices, USA). The fluorescence measurement protocol followed the conclusions of research by Li et al.[21], where excitation was performed at 393 nm, and the fluorescence emission spectrum was measured between 550 and 850 nm. All measurements were performed in a 96-well plate at room temperature. The slit width of the spectrophotometer was set at 20 nm.

Infrared spectrum detection

The Chl and β-Car were mixed to obtain sample A, with Chl concentration at 20.00 mg/L and β-Car concentration at 7.20 mg/L. Samples B (Chl 20.00 mg/L) and C (Car 7.20 mg/L) were also prepared as controls. Infrared detection was performed on these three sample groups. 100 mg of potassium bromide was taken and ground evenly. It was then pressed into a pellet at a pressure of 20 MPa, and the infrared background was

measured. Afterward, 1 mg of the sample was collected with a capillary tube and spread onto the pressed potassium bromide pellet. The coated samples were left to air-dry naturally and were coated 2–3 more times and dried again. After that, the samples were directly subjected to infrared testing using the iS10 FT-IR spectrometer from Thermo Fisher Scientific, USA. The spectral range was set from 400 to 4,000 cm^{-1}. The spectrometer had a resolution of 4 cm^{-1}, a signal-to-noise ratio of 50,000:1, and was scanned 32 times.

Quantum chemical calculations and wave function analysis

The molecular structure's geometric optimization and excited state calculations were performed using Gaussian 16 (A.03) software[22]. In this research, quantum chemical calculations were performed using Density Functional Theory (DFT) in combination with Time-Dependent Density Functional Theory (TD-DFT). The geometric optimization and frequency calculations were carried out using the B3LYP-D3(BJ) functional in combination with the 6-31G(d) basis set. The optimized structures obtained did not exhibit any imaginary frequencies, indicating they were at true energy minima. For the excited state calculations, the CAM-B3LYP-D3(BJ) functional combined with the 6-311G(d,p) basis set was employed. During the quantum chemical calculations of the infrared spectra, using a correction factor of 0.9614 was considered to refine the results at the B3LYP/6-31G* level[23]. The atomic dipole moment correction using Hirshfeld (ADCH) population analysis, hole-electron analysis, and independent gradient model (IGM) analysis was performed using Multiwfn 3.8 software[24,25]. The molecular structure and spectra were visualized using GaussView 6.0 software.

Statistical analysis

The experimental data are presented as the mean ± standard deviation of triplicate readings. The data were subjected to analysis using the Analysis of Variance (ANOVA) function in the SPSS Statistics 21 software. A significance level of $p = 0.05$ is employed, whereby $p < 0.05$ indicates a significant difference. For data visualization and graphing, Origin 2018 software was employed.

Results and discussion

Impact of Car on Chl photostability

Previous studies have indicated that the enhancement of the photostability of Chl through weak interactions can effectively preserve the natural structure of Chl[9,21]. Figure 1 shows the aggregation configuration of Chl *a* and β-Car molecules after performing ab initio molecular dynamics simulations, which validates the rationality of the weak interaction-based aggregation of Chl *a* and β-Car. A structural optimization process revealed that both Chl *a* and β-Car aggregate in a manner that Chl *a* utilizes its phytyl tail and porphyrin ring to encircle the conjugated polyene chain of β-Car. This type of aggregated configuration is designated as the Chl/Car 'embrace' aggregation in this study. *In vitro* assembly studies in aqueous buffer demonstrated that Car can facilitate the self-assembly of Chl into aggregates by enhancing the interactions between the hydrophobic phytyl tails[26]. This aggregation configuration allows for a larger interaction surface area between the weakly polar group of β-Car and the phytyl group of Chl *a*, which

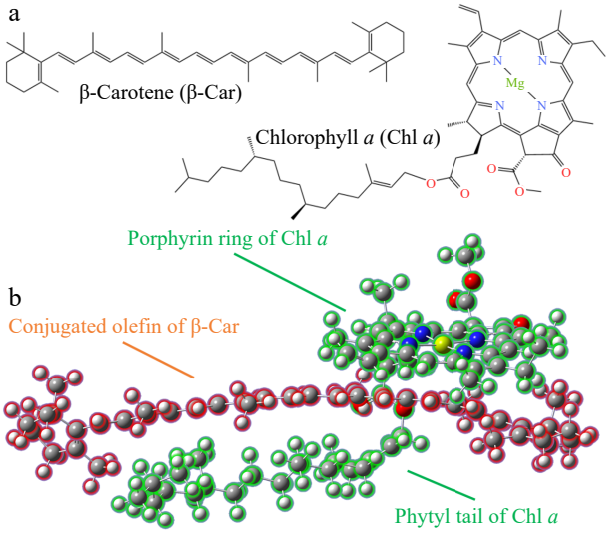

Fig. 1 (a) Molecular structures of Chl and Car. (b) Aggregation configuration of Chl/Car.

contributes to the stability of the aggregate through van der Waals (vdW) forces. It is similar to the stability of the Chl *a* 'sandwich' aggregate observed in previous studies, which is maintained by extensive vdW forces between the phytyl groups[21]. Furthermore, previous studies have demonstrated that car molecules can form complexes with ligand molecules, such as cyclodextrin and glycyrrhetinic acid. These complexes can affect the physicochemical properties of car molecules. Both the cyclodextrin molecule and the glycyrrhizic acid aggregate molecule possess a structure similar to a ring, with a hydrophobic cavity in the center. Due to its hydrophobic property, carotenoid tends to penetrate the hydrophobic cavity when aggregating with molecules of structures like cyclodextrin and glycyrrhizic acid. The aggregation mode in these types of aggregation was facilitated by the ligand molecules by providing a hydrophobic cavity that 'embraced' the Car molecules[27,28].

Figure 2a illustrates the color variations exhibited by the mixture of Car and Chl at varying concentrations following exposure to illumination for 7 d. The concentration of carotenoids increased in a stepwise manner from sample A to F. The F group exhibited the most intense green color after 7 d. Group G demonstrates that without adding Car, the Chl solution underwent significant fading. In group H, the color change of the Car was minimal, indicating its higher photostability. Figure 2b displays the retention of Chl after being mixed with Car and exposed under illumination for 7 d. The retention of Chl correlates with the observed green color in Fig. 2a. As the concentration of β-Car increased, the retention of Chl also increased. In Group F, the retention rate of Chl reached 127.22% in comparison to the control. At this juncture, the molar ratio of Chl to β-Car was 1.66:1. The results indicate that the interaction between Chl and β-Car can enhance the photostability of Chl. It is worth noting that in this system, the ratio of Chl to Car in the range of 1.66 to 10 was similar to the molecular ratio of Chl and Car in the photosynthetic system[29,30]. It was demonstrated that an adequate amount of Chl compared to Car increased the likelihood of interaction between free Chl and Car molecules, which in turn promoted the formation of Chl/Car 'embrace' aggregates.

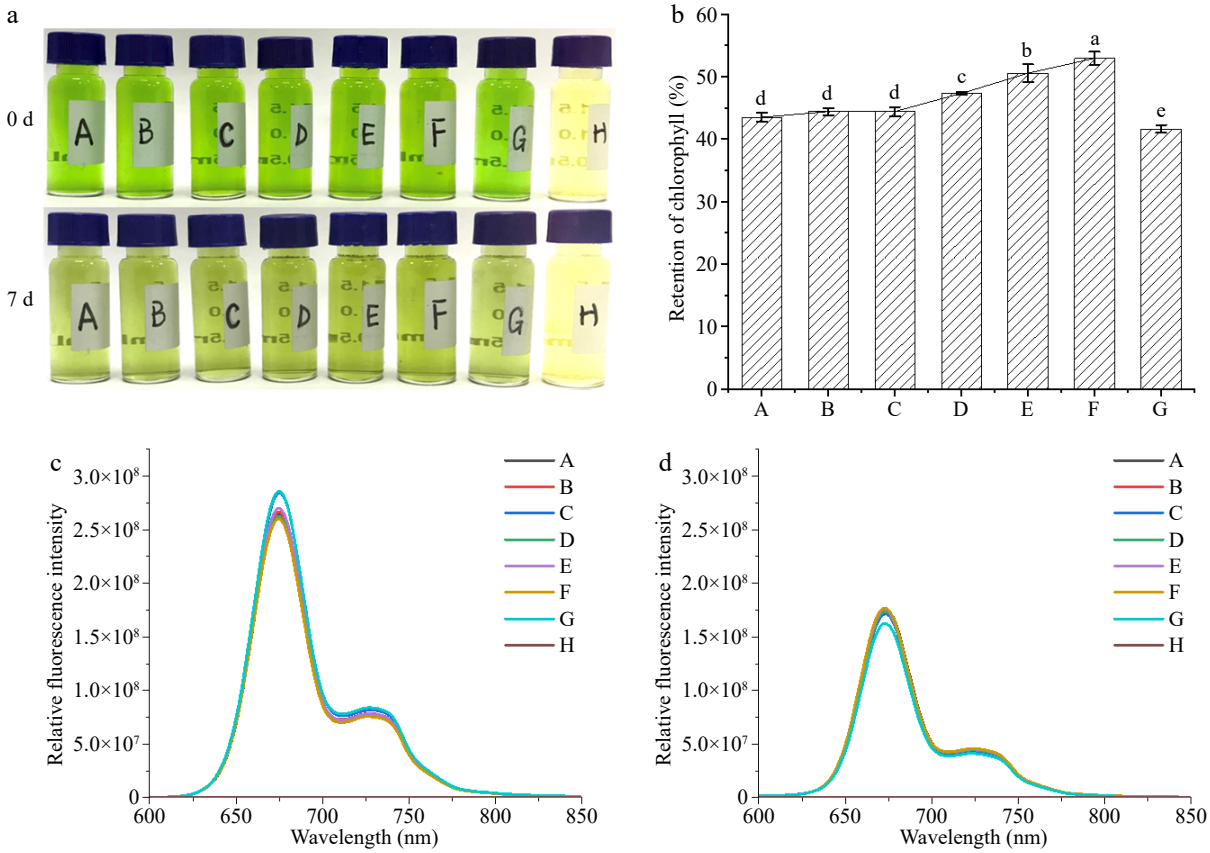

Fig. 2 Changes in Chl/Car mixture exposed for 7 d. (a) Images of samples; (b) retention of Chl; (c) fluorescence emission spectra before light exposure; (d) fluorescence emission spectra after light exposure. (Chl concentrations for samples A, B, C, D, E, F are 19.93 mg/L, and β-Car concentrations are 1.20, 2.40, 3.60, 4.80, 6.00, 7.20 mg/L respectively. G: Chl 19.93 mg/L; H: Car 3.60 mg/L).

Mechanism of Chl/Car interaction

The characteristic fluorescence spectra of Chl's porphyrin ring in the Chl/Car aggregates was analyzed, as shown in Fig. 2c & d. The fluorescence spectra of Chl in different groups exhibit near-complete overlap before and after light exposure. This indicates that the interaction between Chl and carotenoids does not affect the fluorescent fragments, specifically the porphyrin ring of Chl[21]. As observed in the photosynthetic system, the coexistence of Chl and Car serves to expand the range of light absorption wavelengths, rather than mutually restricting the photosensitive groups. At the same time, as illustrated in Fig. 2a & b, the mixing of Chl and Car enhanced the stability of Chl, indicating an interaction between them. The interaction between Chl and Car was observed to occur in the non-photosensitive fragments, which were identified as the side group of Chl. This finding is consistent with the configuration of the 'embrace' aggregate. On the other hand, compared to Fig. 2c, d shows a general decrease in fluorescence intensity. This is attributed to the degradation of Chl under light exposure, resulting in a reduction of fluorescent intensity.

Figure 3a shows the changes in the infrared spectra before and after the mixture of Chl and Car. The generation, disappearance, and shift of characteristic peaks of Chl/Car in comparison to the characteristic peaks of Chl or Car as individual components in the infrared spectrum have been organized and presented in Supplemental Table S1. The main changes in characteristic peaks before and after aggregation of Chl and Car are as follows: 1) The peak of Chl at 669.7 cm^{-1} shifts to 687.23 cm^{-1} after Chl/Car aggregation. 2) The peak of Chl at 1,084.54 cm^{-1} weakens. 3) The peak of Chl at 1,382.1 cm^{-1} shifts to 1,393.88 cm^{-1} after Chl/Car aggregation. 4) All three groups of samples show shifts in peak positions in the range of 3,300–3,400 cm^{-1}. 5) The peak of Car at 3,672.64 cm^{-1} shifts to 3,661.37 cm^{-1} after Chl/Car aggregation. Changes 4) and 5) occur in the range of infrared spectroscopy characteristic areas. Typically, the broad peak between 3,000 and 3,500 cm^{-1} represents hydroxyl or amino groups. The changes in that peak are primarily due to molecular vibrations resulting from overall molecular conformational changes. Therefore, it is not discussed further when studying the molecular interactions in Chl/Car aggregation.

Based on Fig. 3a and the data in Supplemental Table S1, by comparing with the results of quantum chemical calculations, it can be more intuitively and accurately described which vibrations of Chl and Car fragments undergo significant changes before and after aggregation. Therefore, the key molecular fragments involved in Chl/Car aggregation can be determined, as shown in Fig. 3b, c & d. Quantum chemical calculations were conducted to analyze the peak at 669.7 cm^{-1} for Chl in the infrared spectrum and the peak at 687.23 cm^{-1} for the Chl/Car aggregate. The corresponding peaks were obtained at 666.37 cm^{-1} for Chl and 685.29 cm^{-1} for Chl/Car, respectively. The vibrational fragments in the corresponding molecules are shown in Fig. 3b. After mixing Chl with Car, the porphyrin ring of Chl and its connection with the phytyl tail formed an 'embrace' configuration with Car and underwent vibrational changes. This observation proved that these fragments were

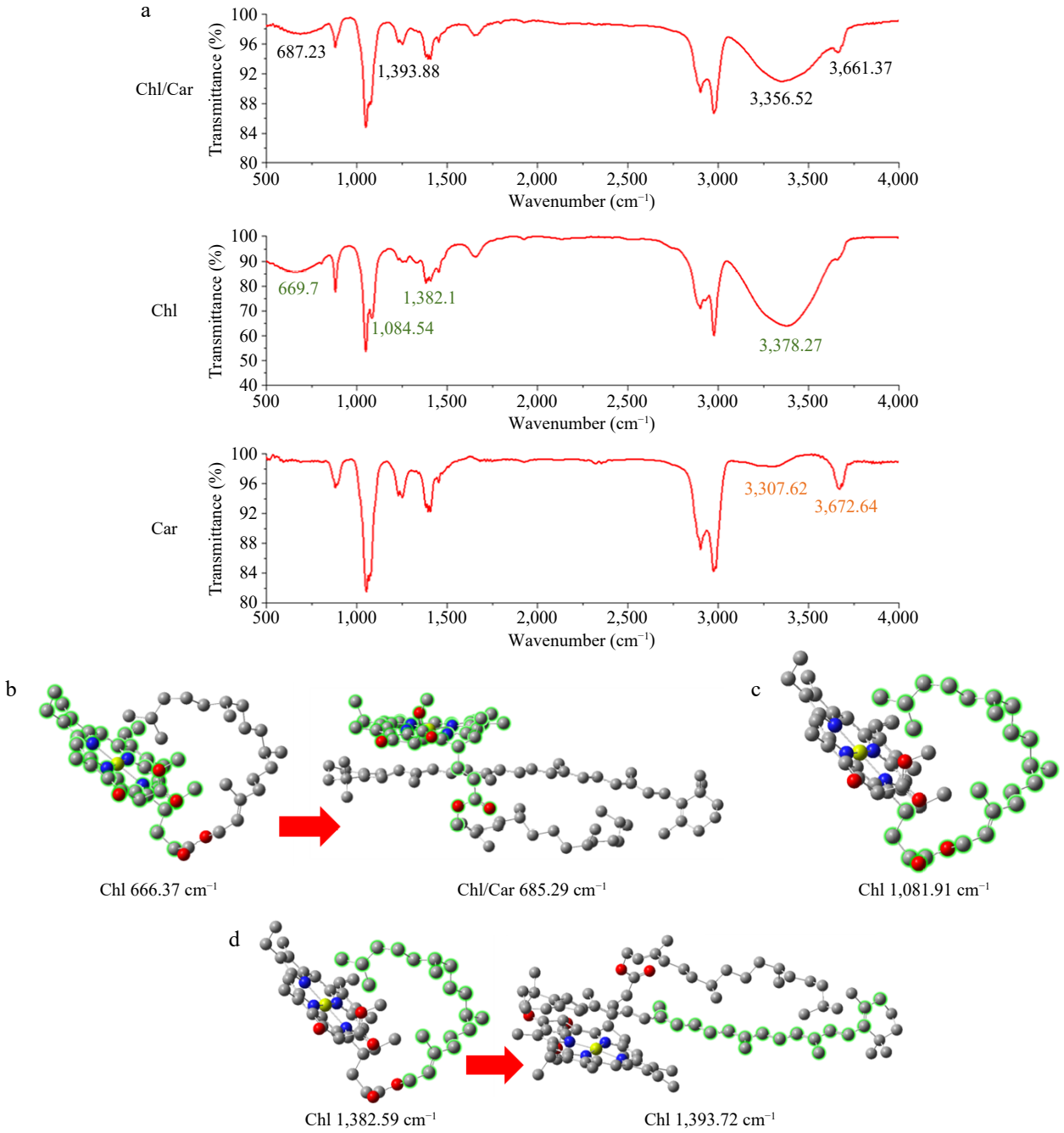

Fig. 3 Changes in infrared spectra before and after mixing Chl and Car. (a) Infrared spectra, (b)–(d) corresponding characteristic fragments vibration.

involved in the interaction between Chl and Car. Quantum chemical calculations were performed to analyze the peak of Chl at 1,084.54 cm^{-1} in the infrared spectrum. The corresponding absorption peak at 1,081.91 cm^{-1} for Chl was obtained, as shown in Fig. 3c. The weakening of the peak at 1,084.54 cm^{-1} after mixing Chl with Car was attributed to the wrapping of the Chl phytyl around the hydrocarbon chain of Car. This leads to the damping of the vibrational mode in that particular fragment. This observation provides evidence that phytyl was involved in the Chl/Car aggregate formation, and the stability of phytyl was enhanced due to the aggregation. The peak of Chl at 1,382.1 cm^{-1} and the peak of the Chl/Car aggregate at 1,393.88 cm^{-1} in the infrared spectrum correspond to the peaks at 1,382.59 cm^{-1} for Chl and 1,393.72 cm^{-1} for the Chl/Car aggregate, respectively, as obtained from quantum chemical calculations. The vibrational fragment is shown in Fig. 3d. In accordance with the previous conclusion, the aggregation of Chl/Car resulted in the interaction between the Car hydrocarbon chain and the Chl phytyl, which rendered the phytyl more stable and the vibration weaker. Based on the analysis mentioned above, the molecular fragments that exhibit significant vibrational changes during aggregation of Chl and Car are confirmed to be the conjugated hydrocarbon chain of Car and the phytyl tail and porphyrin ring of Chl that envelop Car. This

indicates that Chl effectively wrapped around Car, thereby validating the Chl/Car 'embrace' model. The experimental results, when considered alongside the theoretical explanations, provide a comprehensive understanding of the aggregation area of Chl/Car.

The aggregation area of Chl/Car was further validated through IGM analysis. In Fig. 4a, the red portion represents intermolecular forces, while the black portion represents intramolecular forces. In this study, only the intermolecular forces were focused. The concentrated distribution of the red portion near sign (λ_2) ρ = 0 indicates that dispersion forces predominantly governed the interaction between individual molecules in the Chl/Car aggregates. The green area in Fig. 4b visually represents the location where this dispersion interaction existed. By combining the analysis of Fig. 4 with Fig. 3, it can be determined that the aggregation area of the Chl/Car aggregates was between Chl and the conjugated polyene chain of Car. Chl achieved the greatest possible coverage of the Car-conjugated polyene chain by bending its phytyl chain, thereby providing a spatial configuration basis for the extensive van der Waals interaction between Chl and Car. This resulted in the greatest van der Waals interaction between the Chl and Car aggregates, thereby maintaining the stability of the aggregate. This extensive van der Waals interaction is analogous to the interaction observed between the two in the photosynthetic system. The van der Waals interaction between the Chl and the Car enables the efficient transfer of charges between these two components in the photosynthetic system[31].

Photoprotection mechanism of Car against Chl

Figure 5 depicts the evolution of the color and UV-visible spectral characteristics of the Chl/Car mixture following 70 days of continuous exposure to light. The samples labeled as C, G, and H here correspond to the same samples labeled as C, G, and H in Fig. 2. Both C and H have an identical initial carotenoid content, which is 3.60 mg/L. A comparison of the UV-visible spectra of C and G revealed that, following 70 d of exposure, the absorption peaks of Chl at 666 nm in the two groups had become completely overlapped. This indicates that the Chl content in both groups had reached consistency, and there was no longer any difference between the Chl content due to interference from β-Car. A comparison of the spectra of C and H reveals that the characteristic absorption peak (400~550 nm) of Car is completely absent in the Car and Chl mixture after 70 d, with only the characteristic absorption peak of Chl remaining[32]. In contrast, the Car sample without adding Chl still retains a distinct characteristic absorption peak of Car, and the solution appears noticeably yellow. It shows that Chl had a destructive effect on β-Car under light, which indirectly proves

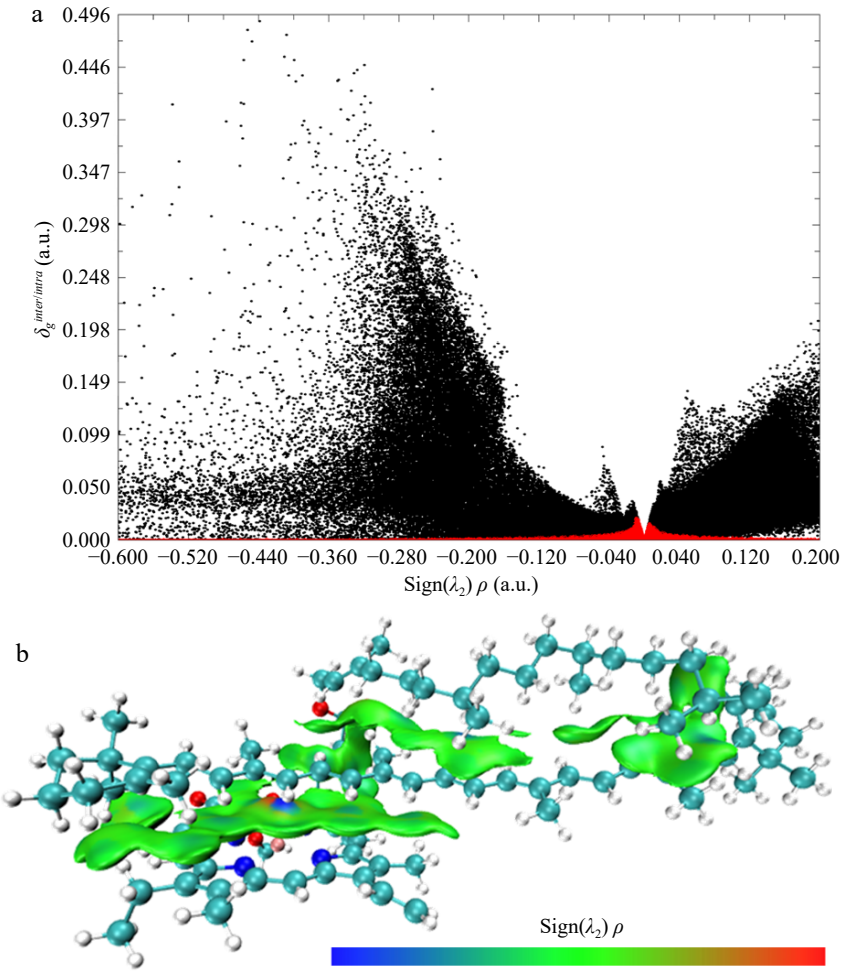

Fig. 4 (a) Scatter plot and (b) schematic diagram of intermolecular interaction of IGM analysis for Chl/Car aggregation (Isovalue = 0.005).

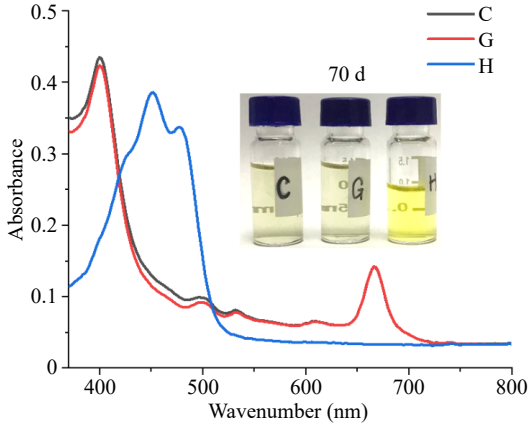

Fig. 5 UV-Vis spectrum of Chl/Car solution exposed for 70 d (C: Chl 19.93 mg/L, β-Car 3.60 mg/L; G: Chl 19.93 mg/L; H: Car 3.60 mg/L).

that the existence of Car was conducive to reducing the destruction of Chl under light and proves that β-Car had a protective effect on Chl. In the photosynthetic system, the interaction between Chl and Car can consume excess energy, thereby maintaining the normal operation of the light system[33]. However, the intricate details of the interactions, including the precise mechanisms of activation, the specific pigments involved, the precise site of dissipation and how the confluence of these factors culminates in the thermal dissipation of excess excitation energy, remain the subject of ongoing debate[34]. In this study, Chl and Car were in a free state when interacting with each other, separated from the photosynthetic system, and the mechanism of interaction between them will be re-examined.

To gain further insight into the mechanism by which Car protects Chl from light, a series of quantum chemical computational experiments were conducted with the objective of providing a detailed explanation of the molecular structure and electronic wave function levels on a microscopic scale. Figure 6a displays the molecular configurations and atomic numbering of Chl *a* and β-Car, with atomic numbers corresponding to the numbers in brackets in Supplemental Table S2. Under normal circumstances, the bond length for a C-C single bond is approximately 1.54 Å, while the bond length for a C=C double bond is around 1.33 Å. By comparing Fig. 6 and Supplemental Table S2, it can be observed that the bond lengths between the inner ring of the Chl porphyrin ring and the conjugated polyene chain of Car are between the bond lengths of C-C and C=C bonds. Furthermore, by analyzing the dihedral angles, it can be inferred that these bonds lie in the same plane, with angles around 0° or 180°. This indicates that these bonds are in a favorable arrangement to form conjugated π bonds. Larger conjugated systems tend to exhibit stronger antioxidant capabilities. This is because larger conjugated systems possess a greater number of delocalized π electrons, which enables them to stabilize and neutralize free radicals and reactive oxygen species, thus reducing oxidative damage more effectively. The Chl porphyrin ring contains eight conjugated bonds, while the Car polyene chain encompasses eleven conjugated bonds. From this perspective, the larger range of conjugated bonds in Car contributes to its ability to possess stronger antioxidant capabilities. This lays the structural foundation for Car's photoprotection of Chl.

The atoms indicated in red in Fig. 6a are electrophilic sites, while the atoms indicated in blue are nucleophilic sites. The specific ADCH charges can be found in Supplemental Table S3. The presence of electrophilic and nucleophilic sites indicates that the atoms at those locations are highly reactive and susceptible to external interference. The active region of Chl is characterised by the presence of a conjugated large π bond range within the porphyrin ring. In contrast, the active region of Car is dominated by the two ends of the conjugated olefin chain, which represent the two ends of the conjugated large π bond. In general, free radicals are predominantly negatively charged and are susceptible to attack by positively charged sites. The destruction of Chl and Car under light is largely attributed to the presence of free radicals[35]. This demonstrates the locations where Chl and Car are readily destroyed by light.

Further analysis of the frontier orbitals of Chl and Car allows for a more visual characterization of the active functional groups. This can be achieved by examining the electron distribution of their respective Highest Occupied Molecular Orbitals (HOMO) and Lowest Unoccupied Molecular Orbitals (LUMO), and the HOMO-LUMO orbital energy gap. In general, a larger HOMO-LUMO orbital energy gap is indicative of a more stable molecule, while a smaller gap is indicative of a less stable molecule. As shown in Fig. 6b, the frontier orbitals of Chl are distributed on the porphyrin ring, while the frontier orbitals of β-Car are distributed on the conjugated polyene chain. This is consistent with our previous judgment. Furthermore, the HOMO-LUMO gap for Chl is 228.311966 kJ/mol, and the HOMO-LUMO gap for β-Car is 212.375695 kJ/mol. This indicates that β-Car has a higher reactivity, indicating that Car is more susceptible to degradation than Chl.

When Chl and Car interact to create Chl/Car aggregates, the impact of external energy on their electronic states serves as a more direct indicator of the protective interplay within these aggregates. Figure 6c shows the schematic diagram of the HOMO-4 to LUMO+4 orbitals of Chl/Car aggregate. The frontier orbitals and neighboring orbitals are primarily distributed alternately on the Chl and Car molecules. This indicates that when the Chl/Car aggregate is excited by lower energy photons, the difference in photon energy can lead to a competitive oxidation relationship between Chl and Car on an overall level. The key point is that in the Chl/Car aggregate, the HOMO corresponds to the orbitals of the Car. This indicates that the conjugated polyene chain of Car within the aggregate is the most easily excited active site. Therefore, when the Chl/Car aggregate is exposed to light, the Car is preferentially excited, providing a protective effect on Chl. This is consistent with the conclusion presented in Fig. 6b that Car is more susceptible to free radical attack due to its lower HOMO-LUMO gap.

Supplemental Table S4 displays the orbitals that contribute the most to the electronic excitation of the five lowest excited states in the aggregate. Because free radicals carry negative charges, they are prone to attack electron-deficient sites after excitation. Through hole-electron analysis, the transfer of electrons can be directly determined in different excited states, thus allowing for an evaluation of the protective relationship between Chl and Car against free radical attacks. In the S1 state, the electrons remain localized on the porphyrin ring, rather than leaving the Chl molecule. In a similar manner, in the S3 state, the electrons do not leave the car molecule but remain

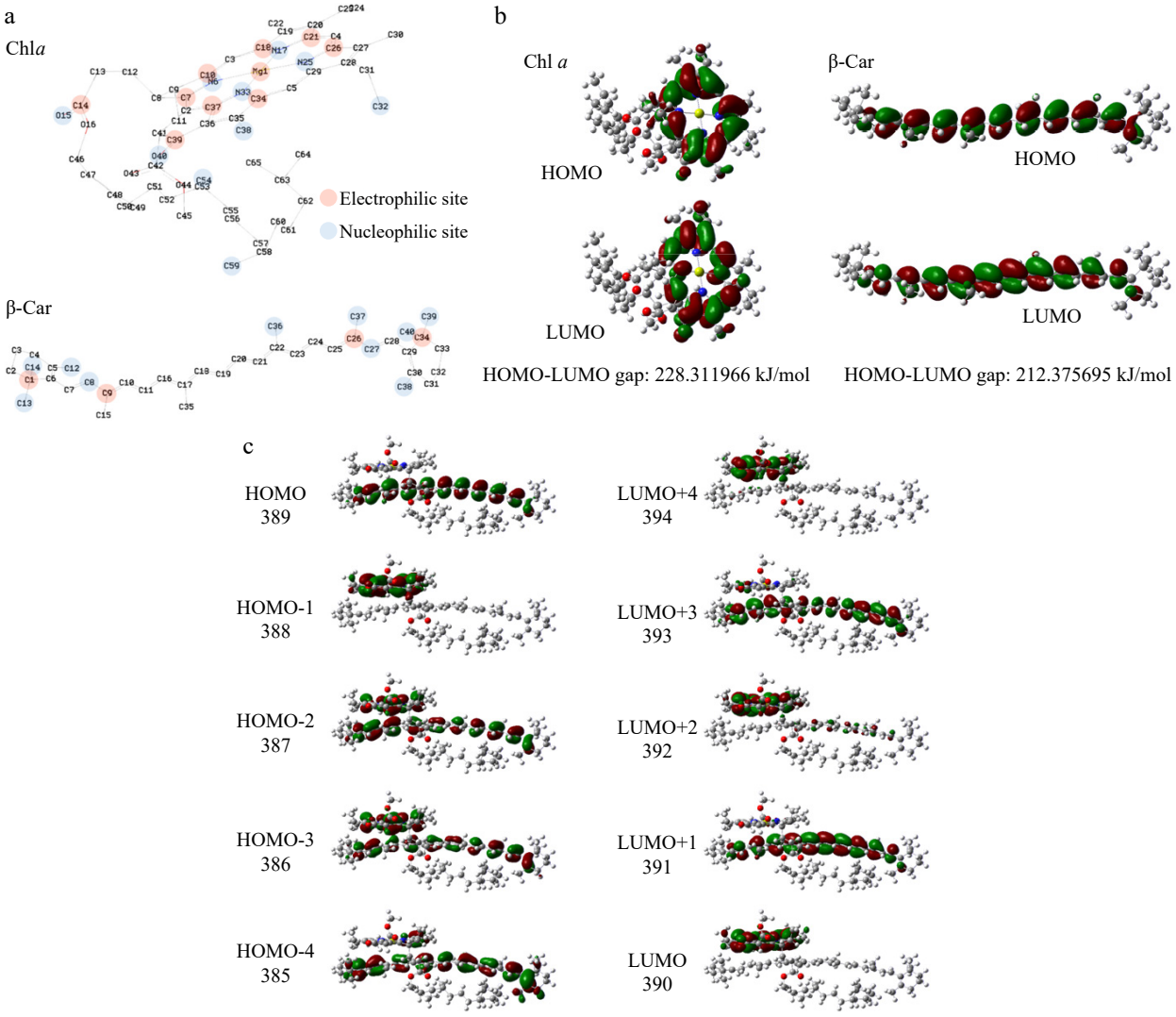

Fig. 6 Reactivity of Chl *a* and β-Car. (a) Molecular configuration, atom number, electrophilic site, nucleophilic site; (b) HOMO-LUMO gap; (c) HOMO-4 to LUMO+4 of aggregate.

localized on the conjugated polyene chain. They all belong to local excitation. Because the electrons do not leave the molecule, local excitation is significantly less affected by external negative-charged free radicals than by positively-charged active groups. In contrast, the charge excitations in S2, S4, and S5 involves charge transfer (CT), where electrons are transferred between Car and Chl. In the lower excited states, such as S2 and S4, the electrons are excited from Car to Chl, while in the higher energy excited state, S5, the electrons are excited from Chl to Car. This indicates that the Car requires lower energy to be excited and dissociate charge, making it more easily generated. It also demonstrates that the core mechanism of Car's photoprotection on Chl lies in the preferential excitation and dissociation of electrons from the conjugated polyene chain of Car, leading to CT. Subsequently, the excited electrons reach the photoreceptive group (porphyrin ring) of Chl, enhancing its protective function against negative charge-free radical attacks. In the photosystem, when Chl and Car molecules are in close contact, the latter will quench the triplet state of the former. The rate of this quenching decreases exponentially as the distance between the two molecules increases. The consequence of the quenching process is the conversion of the Chl molecule from the triplet excited state to the ground state, while the Car molecule undergoes a transition from the ground state to the triplet excited state[36]. The protection mechanism of Car for Chl in the photosystem and the results of this study both reflect that Car has a higher priority in being excited.

Conclusions

To conclude, this research indicates that Car in the Chl/Car mixture enhanced the photostability of Chl. Chl/Car had a 27.22% higher Chl retention rate than free Chl after 7 d of illumination, with a Chl to Car ratio of 1.66:1. The protective effect of Car on Chl in Chl/Car mixtrue was based on an 'embrace' configuration of the aggregate. The conjugated olefin chain of Car created a large-area vdW interaction with the porphyrin ring and bent the phytyl chain of Chl to maintain aggregate stability. The conjugated polyene chain of Car provided the HOMO orbitals of the Chl/Car aggregates, and it has shown that Car supplied electrons in the low-lying excited states S2 and S4, providing direct evidence of Car's high vulnerability within the

aggregates. The findings of this study offer valuable theoretical and technical insights that can directly contribute to the development of liquid Chl drinks. Car, a natural active substance that frequently accompanies Chl, is a viable ingredient for Chl beverages. According to the color of the natural light system, the beverage processing according to the ratio of the two in this study will not bring negative effects on the color of Chl drinks. This study provides a research foundation for improving the color stability of natural food pigments through interactions within aggregates. This allows us to develop more stable and long-lasting natural color formulas, thereby broadening the possibilities for food product design, and enhancing the quality of food products while ensuring consumer health.

Author contributions

The authors confirm contribution to the paper as follows: conceptualization: Li F, Zhang Y; methodology: Li F, Shen S, Yang Z, Zhang J; software: Li F, Yang Z, Zhang J; formal analysis: Li F; investigation: Li F, Shen S; data curation: Shen S, Yang Z, Zhang Y; validation: Shen S; resources: Zhang Y; visualization: Shen S; supervision, project administration, funding acquisition: Zhang Y; writing - original draft: Li F, Ibrahim AN; writing - review & editing: Li F, Zhang Y. All authors reviewed the results and approved the final version of the manuscript.

Data availability

The authors confirm that the data supporting the findings of this study are available within the article and its supplementary materials.

Acknowledgments

This work was supported by the National Natural Science Foundation of China (No. 32072233) and the Natural Science Foundation of Hainan Province (No. 323CXTD381).

Conflict of interest

The authors declare that they have no conflict of interest.

Supplementary Information accompanies this paper at (https://www.maxapress.com/article/doi/10.48130/fia-0024-0021)

Dates

Received 10 April 2024; Revised 2 June 2024; Accepted 19 June 2024; Published online 18 July 2024

References

1. da Silva Ferreira V, Sant'Anna C. 2016. Impact of culture conditions on the chlorophyll content of microalgae for biotechnological applications. *World Journal of Microbiology and Biotechnology* 33:20
2. Li Y, Cui Y, Hu X, Liao X, Zhang Y. 2019. Chlorophyll supplementation in early life prevents diet-induced obesity and modulates gut microbiota in mice. *Molecular Nutrition & Food Research* 63:1801219
3. Queiroz Zepka L, Jacob-Lopes E, Roca M. 2019. Catabolism and bioactive properties of chlorophylls. *Current Opinion in Food Science* 26:94–100
4. Cao J, Li F, Li Y, Chen H, Liao X, et al. 2021. Hydrophobic interaction driving the binding of soybean protein isolate and chlorophyll: Improvements to the thermal stability of chlorophyll. *Food Hydrocolloids* 113:106465
5. Yasuda M, Oda K, Ueda T, Tabata M. 2019. Physico-chemical chlorophyll-a species in aqueous alcohol solutions determine the rate of its discoloration under UV light. *Food Chemistry* 277:463–70
6. Rontani JF, Amiraux R, Smik L, Wakeham SG, Paulmier A, et al. 2021. Type II photosensitized oxidation in senescent microalgal cells at different latitudes: Does low under-ice irradiance in polar regions enhance efficiency? *Science of The Total Environment* 779:146363
7. Özkan G, Ersus Bilek S. 2015. Enzyme-assisted extraction of stabilized chlorophyll from spinach. *Food Chemistry* 176:152–57
8. Zhang Z, Niu L, Li D, Liu C, Ma R, et al. 2017. Low intensity ultrasound as a pretreatment to drying of daylilies: Impact on enzyme inactivation, color changes and nutrition quality parameters. *Ultrasonics Sonochemistry* 36:50–58
9. Li F, Zhou L, Cao J, Wang Z, Liao X, et al. 2022. Aggregation induced by the synergy of sodium chloride and high-pressure improves chlorophyll stability. *Food Chemistry* 366:130577
10. Viera I, Pérez-Gálvez A, Roca M. 2019. Green natural colorants. *Molecules* 24:154
11. Masone D, Chanforan C. 2015. Study on the interaction of artificial and natural food colorants with human serum albumin: A computational point of view. *Computational Biology and Chemistry* 56:152–58
12. Umena Y, Kawakami K, Shen JR, Kamiya N. 2011. Crystal structure of oxygen-evolving photosystem II at a resolution of 1.9 Å. *Nature* 473:55–60
13. Pan X, Liu Z, Li M, Chang W. 2013. Architecture and function of plant light-harvesting complexes II. *Current Opinion in Structural Biology* 23:515–25
14. Pinnola A, Dall'Osto L, Gerotto C, Morosinotto T, Bassi R, et al. 2013. Zeaxanthin binds to light-harvesting complex stress-related protein to enhance nonphotochemical quenching in *Physcomitrella patens*. *The Plant Cell* 25:3519–34
15. Cupellini L, Calvani D, Jacquemin D, Mennucci B. 2020. Charge transfer from the carotenoid can quench chlorophyll excitation in antenna complexes of plants. *Nature Communications* 11:662
16. Hong JE, Lim JH, Kim TY, Jang HY, Oh HB, et al. 2020. Photo-Oxidative Protection of Chlorophyll *a* in C-Phycocyanin Aqueous Medium. *Antioxidants* 9:1235
17. Chmeliov J, Bricker WP, Lo C, Jouin E, Valkunas L, et al. 2015. An 'all pigment'model of excitation quenching in LHCII. *Physical Chemistry Chemical Physics* 17:15857–67
18. Dall'Osto L, Caffarri S, Bassi R. 2005. A Mechanism of Nonphotochemical Energy Dissipation, Independent from PsbS, Revealed by a Conformational Change in the Antenna Protein CP26. *The Plant Cell* 17:1217–32
19. Perwez Hussain S, Harris CC. 2007. Inflammation and cancer: An ancient link with novel potentials. *International Journal of Cancer* 121:2373–80
20. Toprak Aktas E, Yildiz H. 2011. Effects of electroplasmolysis treatment on chlorophyll and carotenoid extraction yield from spinach and tomato. *Journal of Food Engineering* 106:339–46
21. Li F, Cao J, Wang Z, Liao X, Hu X, et al. 2022. Dual aggregation in ground state and ground-excited state induced by high concentrations contributes to chlorophyll stability. *Food Chemistry* 383:132447
22. Frisch MJ, Trucks GW, Schlegel HB, Scuseria GE, Robb MA, et al. 2016. *GAUSSIAN16. Revision C. 01*. Gaussian Inc., Wallingford, CT, USA.
23. Scott AP, Radom L. 1996. Harmonic Vibrational Frequencies: An Evaluation of Hartree–Fock, Møller–Plesset, Quadratic Configuration Interaction, Density Functional Theory, and Semiempirical Scale Factors. *The Journal of Physical Chemistry* 100:16502–13

24. Lu T, Chen F. 2012. Multiwfn: A multifunctional wavefunction analyzer. *Journal of Computational Chemistry* 33:580−92
25. Liu Z, Lu T, Chen Q. 2020. Intermolecular interaction characteristics of the all-carboatomic ring, cyclo[18]carbon: Focusing on molecular adsorption and stacking. *Carbon* 171:514−23
26. Alster J, Polívka T, Arellano JB, Chábera P, Vácha F, et al. 2010. β-Carotene to bacteriochlorophyll c energy transfer in self-assembled aggregates mimicking chlorosomes. *Chemical Physics* 373:90−97
27. Mele A, Mendichi R, Selva A. 1998. Non-covalent associations of cyclomaltooligosaccharides (cyclodextrins) with *trans*-β-carotene in water: evidence for the formation of large aggregates by light scattering and NMR spectroscopy. *Carbohydrate Research* 310:261−67
28. Polyakov NE, Leshina TV, Salakhutdinov NF, Kispert LD. 2006. Host−guest complexes of carotenoids with β-glycyrrhizic acid. *The Journal of Physical Chemistry B* 110:6991−98
29. Wei X, Su X, Cao P, Liu X, Chang W, et al. 2016. Structure of spinach photosystem II–LHCII super complex at 3.2 Å resolution. *Nature* 534:69−74
30. Xiaodong S, Mei L. 2021. Advances in structural biology of photosystem complexes in higher plants. *Chinese Journal of Nature* 43(3):165−75
31. Polívka T, Sundström V. 2004. Ultrafast dynamics of carotenoid excited states−from solution to natural and artificial systems. *Chemical Reviews* 104:2021−72
32. Pšencík J, Arellano JB, Collins AM, Laurinmäki P, Torkkeli M, et al. 2013. Structural and functional roles of carotenoids in chlorosomes. *Journal of Bacteriology* 195:1727−34
33. Magdaong NCM, Blankenship RE. 2018. Photoprotective, excited-state quenching mechanisms in diverse photosynthetic organisms. *Journal of Biological Chemistry* 293:5018−25
34. Govindjee U. 2014. *Non-photochemical quenching and energy dissipation in plants, algae and cyanobacteria*. Dordrecht: Springer Netherlands. https://doi.org/10.1007/978-94-017-9032-1
35. Rontani JF, Aubert C. 1994. Effect of oxy-free radicals upon the phytyl chain during chlorophyll a photodegradation. *Journal of Photochemistry and Photobiology A: Chemistry* 79:167−72
36. Yakovlev AG, Taisova AS. 2024. Quenching of bacteriochlorophyll a triplet state by carotenoids in the chlorosome baseplate of green bacterium *Chloroflexus aurantiacus*. *Physical Chemistry Chemical Physics* 26:8815−23